Low thermal budget photonic processing of highly conductive Cu interconnects based on CuO nanoinks: Potential for flexible printed electronics

Matthew S. Rager[a], Tolga Aytug[a,b,], Gabriel M. Veith[a], and Pooran Joshi[a,*]*

[a]Oak Ridge National Laboratory, 1 Bethel Valley Rd, Oak Ridge, TN 37831-6061

Abstract

In the developing field of printed electronics nanoparticle based inks such as CuO show great promise as a low-cost alternative to other metal-based counterparts (e.g., silver). In particular, CuO inks significantly eliminate the issue of particle oxidation, before and during the sintering process, that is prevalent in Cu-based formulations. We report here the scalable and low-thermal budget photonic fabrication of Cu interconnects employing a roll-to-roll compatible pulse-thermal-processing (PTP) technique that enables phase reduction and subsequent sintering of inkjet-printed CuO patterns onto flexible polymer templates. Detailed investigations of curing and sintering conditions were performed to understand the impact of PTP system conditions on the electrical performance of the Cu patterns. Specifically, the impact of energy and power of photonic pulses on print conductivity was systematically studied by varying the following key processing parameters: pulse intensity, duration and sequence. Through optimization of such parameters, highly conductive prints in < 1 s with resistivity values as low as 100 nΩ m has been achieved. It was also observed that the introduction of an initial ink-drying step in ambient atmosphere, after the printing and before sintering, leads to significant improvements in mechanical integrity and electrical performance of the printed Cu patterns. Moreover, the viability of CuO reactive inks, coupled with the PTP technology and pre ink-drying protocols, has also been demonstrated for the additive integration of a low-cost Cu temperature sensor onto a flexible polymer substrate.

Keywords: Inkjet printing, CuO nanoparticle ink, pulsed thermal processing, photonic sintering

[b] Also with: University of Tennessee, 401 Nielsen Physics Building, 1408 Circle Drive, Knoxville, TN 37996

INTRODUCTION

Recent advancements in inkjet printing have introduced a new era in the fabrication of thin, flexible electronics using metal-nanoparticle-based (NP) inks. Inkjet technology enables printing of finely detailed patterns, down to the micron scale, onto a variety of flexible substrates including plastic[1], paper[2,3], rubber, and fabric for applications in sensor technology[4], RFID tag antennas[5], solar cells[6] and many other fields[7]. In addition, as an additive technology, inkjet printing shows promise for green manufacturing with significantly reduced material waste and as cost-effective alternative to fabrication methods such as sputtering, screen printing, and lithography [8]. Moreover, it can be readily implemented into large-scale production methods (e.g. roll-to-roll manufacturing, R2R), for the rapid fabrication of high-definition electronic components[9,10]. In fact, a recent IDTechEx report in which the innovations in ink formulations, printing technology, and manufacturing practices were highlighted, forecasts that the worth of printed, flexible, and organic electronics industries will more than double by 2025[11]. Currently, silver-based NP inks are commonly preferred in printed technologies because of their high conductivity and high oxidation resistance. However, these inks are not economical and typically require long sintering times that are not conducive for applications requiring low-temperature compatible substrates[12]. On the other hand, Cu-based NP inks offer a cost-effective alternative, at only a few percent of the cost of silver inks[13], but the issues related to oxidation of Cu before and/or during printing make it essential to store and sinter the ink under inert atmospheres[14]. Solutions to this critical issue have been explored by encapsulating Cu particles in protective metal shells (e.g., silver and gold)[15], in organic capping agents[16], and/or by using CuO NPs dispersed in solvents containing a reducing agent[17]. The former approach requires complicated and expensive processing steps, while relatively easily formulated organically-shelled inks have not yet reached conductivity levels high enough to satisfy application requirements. Of the approaches cited above, the last - CuO NPs dispersed in reducing solvents - offers a unique solution not only to circumvent the oxidation problem but also, when coupled with photonic sintering techniques such as pulse-thermal-processing (PTP), enables relatively facile implementation into industrial-scale fabrication.

Conventional post-printing processing of silver inks is typically achieved by thermal sintering using a hotplate or an oven at temperatures reaching to 300 ^{o}C and durations up to a few hours. However, this conventional approach is not feasible for CuO-based inks because the

rate of oxidation is higher than the rate of chemical reduction to elemental Cu, which necessitates sintering to be performed in an inert atmosphere[18]. In addition, polymer based substrates having low glass transition temperatures, such as polyethylene terephthalate (PET) or polyethylene naphthalate (PEN), easily degrades during the thermal processing[19]. To overcome these common problems, more selective sintering approaches such as laser-beam and PTP methods have been developed. In both cases, printed samples are irradiated with high-intensity photons by flashing light in successive pulses at a given frequency. The duration of light exposure per pulse typically ranges from microsecond to a few milliseconds. The combination of high intensity and short duration irradiation heats the thin print pattern (typically < 5μm in thickness) to the desired sintering temperatures, while simultaneously preventing decomposition of the substrate and enabling chemical reduction of CuO ink[20]. Among these methods, the PTP technique is especially attractive for mass production due to its ability to sinter large-scale prints at high speeds (when coupled with R2R design) in comparison to complex, expensive, and relatively smaller area limited laser sintering approach[21].

In the present study, we have investigated the chemical reduction and sintering of CuO NP inks using a high intensity flash lamp PTP system to obtain conductive Cu interconnects on flexible polymer substrates. The PTP operating parameters such as pulse intensity, pulse duration, and the number of pulses were systematically screened to control the energy and power output of the system for the optimization of print performance, while maintaining the substrate integrity. The influence of the processing protocols on the re-oxidation evolution of sintered samples as well as the importance of a drying step, prior to sintering, on the electrical performance of printed patterns was reported. The viability of the present approach has also been demonstrated through fabrication of a Cu resistor pattern to function as a temperature sensor device.

EXPERIMENTAL DETAILS

Inkjet Printing

A Dimatix DMP-2831 inkjet printer (Fujifilm) was used to print 16 wt.% water-based CuO ink (Novacentrix, ICI-002HV) an average particle size of 126 nm onto silica-coated PET substrates (Novacentrix, Novele™ IJ-220), on which the silica coating provides a porous

morphology for improved droplet absorption and wetting[22]. The CuO ink has a viscosity around 9-12 cPs, and fits the recommended viscosity parameters (10-12 cPs) provided by the printer manufacturer. The printer cartridge utilizes a micro-electro-mechanical system based piezo controlled nozzle to jet out highly controlled droplet volumes. In the present study, we have used a 10 picoliter ink-cartridge that produces ~30 µm diameter droplets. Nozzle voltages and jetting waveforms were adjusted to achieve a drop velocity of 7-8 m/s. Drop spacing was kept constant at 20 µm to produce slightly overlapping print lines to eliminate the potential gaps between the tracks. We engineered the jetting waveform to eradicate the formation of satellite droplets, which create inconsistent droplet volumes and have been shown to cause issues in print uniformity[23].

Pulse Thermal Processing (PTP)

A PulseForge 3300 (Novacentrix) system was employed to reduce insulating CuO prints to conductive Cu interconnects. The R2R compatible PulseForge system uses an intense-pulse lamp that irradiates samples with a high energy light mapping the UV-Vis spectrum. The curing conditions of the CuO inks were systematically optimized by adjusting the system parameters including capacitor bank voltage, number of pulses, and pulse duration. These parameters control the peak power and energy exposure output of the system. The samples are processed in a stationary configuration (i.e., not in R2R mode) due to a wide exposure zone covering the entire sample. An illustration of the CuO nanoink sintering in an envisioned R2R PTP configuration is shown in Fig. 1. For curing the inks, bank voltages, number of pulses, and pulse durations were varied in the range of 150-300V, 2-30 pulses, and 1.5-6 ms, respectively. The repetition rate for multiple pulses was set at 1.8 Hz, corresponding to a 0.555 s delay between each pulse. The upper power limit for curing the CuO patterns was defined by the damage threshold of the silica-coated PET substrates.

Characterization

The electrical performance of the printed Cu patterns was evaluated in terms of the electrical conductivity and sheet resistance characteristics. The electrical resistance measurements were taken with a Fluke multimeter and the sheet resistance measurements were acquired with a Jandel RM3 four-point probe. The surface morphology of the samples was analyzed using a Hitachi S-4100 high-resolution field-emission type scanning electron microscope. X-ray

photoelectron spectroscopy (XPS) data was collected to examine the reduction of CuO phase to Cu using a PHI 3056 spectrometer with an Al anode source operated at 15 kV and an applied power of 350 W. Adventitious carbon and the carbon from the PET substrate was used to calibrate the binding energy shifts of the samples (C1s = 284.4 eV). High resolution data was collected at pass energy of 23.5 eV with 0.05 eV step sizes and a minimum of 60 scans were acquired to improve the signal to noise ratio. The thickness of the prints (~ 0.7µm) was determined by a surface profilometer (Alpha-Step IQ). Temperature profiles of the CuO films were simulated using the SimPulse software provided by Novacentrix.

Resistive temperature sensor fabrication

A copper resistor pattern was printed onto a PET substrate to function as a flexible temperature sensor. Silver epoxy contacts were used to conduct resistance measurements using a multimeter, while the sample was being kept in an environmental chamber. The resistance of the device was documented at room temperature before the oven temperature was manually raised from 30 ^{o}C to 100 ^{o}C at increments of 10 ^{o}C. Resistance values were recorded 10 min after the temperature stabilized at each set-point.

RESULTS AND DISCUSSION

PTP is a low-thermal budget, i.e. low process temperatures and very short process times, technique suitable for integration on temperature sensitive substrates. PTP offers the following key process parameters - pulse power, pulse number, and pulse duration and sequence - for effective low temperature curing and sintering of thin films printed or deposited on flexible templates. For clarity, we define curing as the process in which the excess solvent is evaporated; organic decomposition is occurred, and CuO NPs are reduced to Cu NPs. Sintering ensues when the energy of the photonic lamp is high enough to enable material diffusion to form a conductive Cu sheet. These processes are schematically displayed in Fig. 2. Figure 2a illustrates the "as-printed" wet state of the film where the CuO particles are dispersed in the solvent. After evaporation of the solvents, separation between the particles decreases leading to agglomeration (Fig. 2b). This enhances the spreading of thermal energy throughout the film matrix, creating a well-connected print after sintering. As the print is irradiated, starting from the film surface, a photo-chemical reduction reaction takes place, where the CuO particles transform into Cu

particles. At this stage, the irradiated energy from the flash lamp must be high enough for the print to reach temperatures that are sufficient for activation of the reduction mechanism[17]. With further increase in thermal energy, sintering takes place resulting in particle growth and particle fusing (Fig. 2c)[20]. Through time the film becomes completely sintered and a conductive sheet is created, where the conductivity is typically described by percolation theory[14].

In the present work, we have observed that the electrical/mechanical performance of printed Cu patterns strongly depends on the curing step involving a combination of drying conditions of CuO nanoinks and subsequent PTP treatment protocols. A delay period between printing and sintering allows excess solvents to diffuse through the porous structure of the coated-PET substrate[24]. Thorough removal of low-boiling-point solvents, such as water, before sintering is critical to prevent delamination as well as to minimize pore formation generally caused by rapid 'explosive' evaporation. Figure 3 shows the impact of pre-sintering drying time in ambient atmosphere (22 ^{o}C, 48% relative humidity) on the electrical performance of the Cu-interconnects. Clearly, drying time dictates the PTP conditions for optimum electrical performance. Samples processed directly after printing using up to 8 photonic pulses showed a very high resistance value exceeding 10^6 Ohms, indicating incomplete reduction/sintering. As the number of pulses was increased, the resistance values decreased substantially to levels below 10 Ohms. Irrespective of the number of photonic curing pulses, for the investigated range of drying times (i.e., 20 - 40 mins), the strong impact of the drying step on the electrical performance of the printed patterns was evident as the resistance values of the samples remained below 100 Ohms. The observed results clearly demonstrated the possibility of achieving a six orders of magnitude increase in print conductivity with fewer pulses and lower energy exposure using a drying step prior to PTP processing. It is noteworthy that the mechanical strength of the films is also influenced by the drying step. All the samples sintered after the incorporation of the drying step showed improved adhesion to the substrate, even after bending at an angle of ~120^{o}. Note that the influence of primary PTP control parameters on the electrical properties of the prints is discussed below.

Oxidation of Cu under normal atmospheric conditions presents significant challenges for various thin film applications. In particular, for electronic devices, formation of native insulating oxides such as CuO and Cu_2O on the patterned film surface substantially degrades the desired electrical properties of the prints. In order to circumvent this issue a protective passivation layer

can be employed[25], increasing the overall process complexity and cost. If the Cu prints can be made environmentally stable through optimization of the processing protocols, the need for protective coatings can be avoided and a lower cost/performance ratio can be attained. Hence, the influence of the removal of solvent(s), before PTP sintering, on the post-oxidation characteristics of the sintered print surfaces is investigated by means of monitoring the changes in the resistance of the samples. Figure 4 compares the electrical performance of the Cu prints, pre-dried at various conditions, as a function of post-exposure time to ambient air. Note that all samples are sintered with the same PTP parameters. Resistance values of the three samples processed after different drying periods were measured over a one week period. While all samples initially demonstrate low-resistance values (~1 Ω), both the undried and the PTP-dried samples showed an increase in resistance only after one day of exposure to ambient air. On the other hand, the resistance of the air-dried sample (~24 hrs) remained virtually unchanged even after five days of exposure. At longer exposure times (> 5 days), while the resistance of the undried as well as PTP-dried samples increased rapidly with time, being more prominent for the former (by a factor of 12), the air-dried sample began to show some degradation in its conductivity only after seven days of exposure. In addition to the electrical performance, mechanical properties of the films were also significantly affected by the pre-drying conditions as can be clearly visualized from the photographs presented in Fig. 4. After one week in ambient atmosphere, the color of the undried (Fig. 4a) and PTP-dried (Fig. 4b) prints not only turned to dark-brown, signifying re-oxidation of the Cu, but the films also showed significant delamination when flexed. In contrast, the air-dried sample retained its bright orange color and flexibility without any visible delamination. This contrasting behavior is most likely associated with the microstructure of the print-pattern prior to sintering. The evaporation of organic solvents from the film matrix during drying, prior to PTP sintering, most likely enhances the diffusion of Cu species during the sintering process, leading to efficient particle growth and coalescence. This in turn enables relatively dense, uniform, environmentally stable, and mechanically robust Cu prints.

The efficient curing and sintering of printed Cu interconnects is dependent on the following two primary PTP control variables - energy exposure and peak power – which were investigated to identify the optimum PTP process space for CuO nanoinks. Hence, the effect of the number of consecutive pulses and corresponding total energy exposure on the electrical conductivity of

printed samples was explored next. The relationship between photonic energy exposure and peak power was used to determine the threshold at which CuO ink is reduced and sintered. The total energy exposure is a function of the peak power, which can be expressed by the following equation,

$$E_{exposure} = \int_0^t P_{peak} \cdot dt$$

where t is the total lamp light exposure time, P_{peak} is the peak power (kW/cm^2) controlled by capacitor bank voltage, and $E_{exposure}$ is the total energy exposure (J/cm^2). The latter is defined as the total lamp irradiance and depends on the number of pulses and pulse duration. Figure 5 compares the influence of pulses number on the Cu print resistance at two controlled peak power values in terms of changes in the sheet resistance characteristics of the samples. Using a peak power of 0.89 ± 0.04 kW/cm^2, the sheet resistance values first showed a gradual drop with increase in the number of pulses reaching a lowest value of 144 mΩ/□ (resistivity ~100 nΩ m) (corresponding to a total $E_{exposure}$ of 27.9 J/cm^2) before showing a rising trend with further increase in number of pulses (Figs. 5a and b). Note that the samples processed for less than 10 pulses or more than 30 pulses were typically under-sintered or over-sintered, respectively, demonstrating excessively high sheet resistance values. In contrast, significantly fewer pulses and lower total energy exposure were needed to reach comparable sheet resistance values when the peak power was slightly increased to 1.2 ± 0.1 kW/cm^2 (Figs. 5c and d). At this higher power level, the samples processed with 3 to 8 pulses (5.06 J/cm^2 - 24.7 J/cm^2) were well-sintered and showed similar sheet resistance values. This indicates that as few as 3 pulses are sufficient to properly sinter samples compared to ~15 pulses needed in the case of the lower power level. The observed sintering characteristics demonstrate a wide process window available with the PTP technique depending on the ink and substrate characteristics. It would be possible to further reduce the thermal budget by optimizing the P_{peak} in combination with the number of photonic pulses required to achieve high electrical performance.

However, note that while the total $E_{exposure}$ budget decreases as the P_{peak} increases, there is a limit to operation at a material specific maximum power before substantial damage to the specimens occurs. That is, pulsing too much of energy in a short amount of time results in complete delamination of the ink layer from the substrate. Since it was realized that the fine tuning of the P_{peak} is crucial for optimization of the PTP sintering conditions, its effect on the

electrical performance of the samples was studied in detail to further gauge the sintering threshold (Fig. 6). During the measurements, the P_{peak} was varied from 0.7 kW/cm^2 to 2 kW/cm^2, while the $E_{exposure}$ and number of pulses were kept constant at 10 J/cm^2 and 2, respectively (see Fig. 5). It is evident from Fig. 6 that the optimal processing window of CuO prints mapped a range of 1.0 kW/cm^2 - 1.8 kW/cm^2. Patterns processed at power levels below 0.7 kW/cm^2 were not sintered at all, and power levels above 2 kW/cm^2 resulted in complete delamination. The highest conductivity was achieved at a P_{peak} of 1.3 kW/cm^2. These conditions can be put into perspective for commercial manufacturing practices considering two pulses with millisecond long duration and a delay of 0.555 s in between them leads to a sub-second sintering time that is well suited for integration into high-throughput R2R manufacturing.

Next the influence of pulse duration on the electrical performance of the Cu prints was investigated (Fig. 7). Note that the number of pulses allows user to change the $E_{exposure}$ in large steps whereas the pulse duration enables fine tuning of the energy exposure. Referring back to Fig. 6, optimum print conductivity was achieved with 2 pulses at a P_{peak} value of 1.3 kW/cm^2. Using these parameters, for the investigated pulse duration range of 2 - 3 ms, patterns exposed to 2 ms radiation showed very high resistance values > 10^8 Ω, consistent with incomplete reduction and sintering of the CuO ink. On the other hand, a slight increase in pulse duration to 2.5 ms (corresponding to an $E_{exposure}$ of 6.7 J/cm^2) resulted in substantial drop of the resistance value to ~ 8 Ω. The resistance of the prints continually decreased in the investigated pulse-width range (see inset); and a low value of 1Ω was obtained at 3 ms duration ($E_{exposure}$ of 7.54 J/cm^2). Consistent also with Fig. 5c and d, the initial drop in resistance at 6.7 J/cm^2 indicates more or less complete reduction of CuO to Cu and partial sintering of the printed pattern. Note that, while reduction and sintering processes occur nearly simultaneously, their optimal energy threshold values are slightly different. In fact, simulated temperature profiles (see Fig. S1 in the supporting document) of the same samples reported in Fig. 7 indicated that the photo-thermal reduction of CuO takes place when the film temperature reaches around 250-270 ^{o}C. As the irradiation time increases, the film absorbs more heat, where temperature rises to ~ 290 ^{o}C, leading to a well-sintered material. These observations corroborates well with the previous reports obtained on elemental Cu-based inks[20]. The sintering ability of PTP on the CuO patterns was further characterized by SEM analysis. Figures 8a and b show SEM images of an as-printed and a photo-sintered sample (the same sample as presented in Fig. 6; processed at P_{peak}= 1.3 kW/cm^2

having a resistance value of 0.75Ω). There is a stark contrast between the CuO ink and the sintered Cu film surface morphologies. While the as-printed sample surface consists of porous and disconnected fine grains, the sintered sample displays a much denser reticulated surface structure having larger size features associated with neck formation accompanied by grain growth[26]. The respective photographs of the as-printed CuO and sintered Cu patterns are included as an inset in Figs. 8a and b. The reduction of CuO to Cu is clearly accompanied by a color change from dark brown to bright orange. To gain further insight into the reduction mechanism, XPS analysis was conducted on as-printed as well as on sintered films. The data collected, as shown in Fig. 9, for both samples (in Cu 2p region) clearly verifies the complete reduction of CuO into Cu phase. Before sintering, the printed film shows the presence of 5 peaks with binding energies of 933.6, 942.0, 944.1, 953.6, and 962.7 eV. This configuration of species is indicative of a Cu^{2+} layer where the 933.6 and 952.6 eV moieties are due to the Cu $2p_{3/2}$ and Cu $2p_{1/2}$ photoelectrons, respectively, while the three other peaks are shake-up lines from the 3d electrons going to a $2p^5$-$3d^9$ type of configuration [marked with "S"]. The intensity ratio of the 942 and 944.1 eV shake-up lines are indicative of a Cu_2O phase instead of a Cu^{2+}-OH chemistry[27]. After the PTP induced reduction, there is a 1 eV shift in the Cu $2p_{3/2}$ species to 932.7 eV along with a complete loss of shake-up lines indicating the formation of metallic Cu^o. In addition, the separation between the Cu $2p_{3/2}$ and Cu $2p_{1/2}$ photoelectron lines (19.8 eV) is also consistent with the presence of Cu^o in the sintered layer. It is noteworthy that the short sintering time not only inhibits re-oxidation of the Cu print[17] but also prevents the underlying low-melting-point polymer substrate from being damaged. High intensity of the flash-lamp and short duration of the radiation pulses heats the film to temperatures high enough to only sinter the nanoparticles but not to the level of melting or decomposing the substrate[20]. In fact, a comparison of the SEM images of the uncoated PET substrate before (Figs. 8c) and after (Fig. 8d) the PTP processing, using the same sintering parameters, reveals virtually no change in their surface structures, further signifying the excellent suitability of the PTP technique for printed electronics applications employing temperature sensitive flexible substrates.

Flexible and printed sensors based on conductive inks offer to meet the cost/performance demands of R2R manufacturing technology. To illustrate the potential utility of the PTP sintered CuO inks in printed electronics applications, resistive temperature sensors were printed and characterized on flexible substrates (see inset of Fig. 10). Resistance temperature sensors work

on the principle of resistance change in a metal, when heated, due to increased collisions of electrons with the atomic vibrations. The relationship between resistance and temperature for different materials can be expressed in terms of the temperature coefficient of resistance (α) using the following equation: $\alpha = \frac{1}{R_o} \cdot \frac{\Delta R}{\Delta T}$, where R_o is the resistance at a reference temperature, ΔR is the change in resistance corresponding to a change in temperature, ΔT. In the present study, the temperature dependence of resistance was evaluated in the range of 30-100 °C as shown in Fig. 10. The sensor resistance values showed a linear dependence with respect to the temperature; which is consistent with the behavior of a bulk Cu in the same temperature range. Accordingly, the calculated temperature coefficient of resistance, $\alpha_{\text{printed Cu}} = 0.00329\ /^{o}C$, is also on-par with that of bulk Cu($\alpha_{\text{bulk Cu}} = 0.00386\ /^{o}C$) at the same $R_o = 20\ ^{o}C$[28]. The slightly lower α for the present ink-jet printed device can be attributed to electron scattering at grain boundaries[29]. The observed printed sensor performance underscores the viability and potential of nanoparticle based reactive inks coupled with R2R compatible high intensity photonic sintering technique for low-cost, large-scale production of thin film sensors and devices, especially on polymeric platforms.

CONCLUSION

In summary, highly conductive and reliable (both environmentally and mechanically) printed Cu interconnects have been processed on flexible PET substrates by exploiting inkjet printing and low thermal budget, PTP technique. Efficient reduction of reactive CuO nanoparticle inks to conductive Cu patterns as well as synergistic relationship between the sintering efficiency and the electrical performance of the printed patterns has been achieved through detailed investigations of light irradiation conditions (energy density, pulse number, pulse duration, P_{peak}, E_{exposure}). Among those P_{peak} and E_{exposure} were the most dominant factors in influencing the Cu-line conductivity and process thermal budget. In addition, drying of excess solvents by introducing a pre drying-step, before curing/sintering, was also found to provide significant enhancement in both the electrical conductivity and the mechanical/environmental stability of the prints. Through optimization of such parameters, it was possible to obtain highly conductive prints in < 1 s with resistivity values as low as 100 nΩ m. The observed electrical performance of the samples was corroborated with the XPS analysis which revealed an efficient reduction of

CuO to Cu at low thermal budgets. The device feasibility of printed Cu patterns was demonstrated through the design of a resistive temperature sensor. The printed resistor showed a stable temperature response with a temperature coefficient of resistance comparable to that of the bulk Cu. Overall, the observed performances of the printed Cu patterns and the resistive temperature sensor element demonstrate a path towards the realization of a flexible sensor platform exploiting a combination of additive inkjet printing and low thermal budget PTP technology.

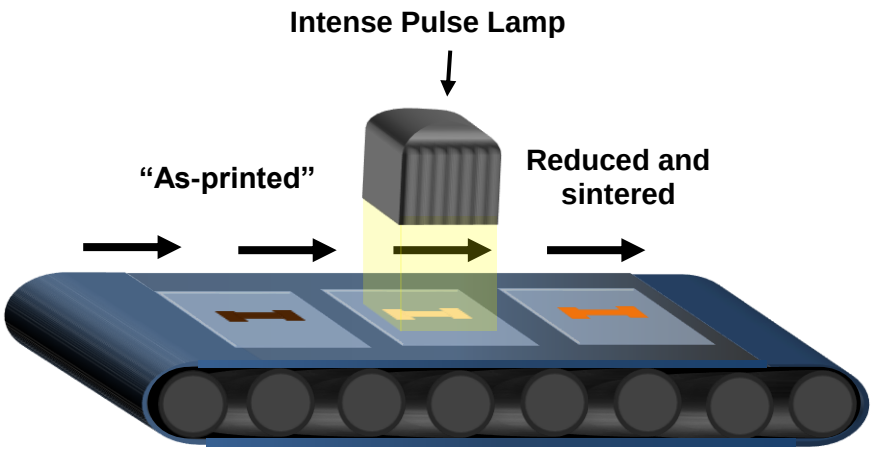

Figure 1. Schematic of R2R pulse-thermal-processing of CuO nanoparticle inks for the production of highly conductive Cu prints.

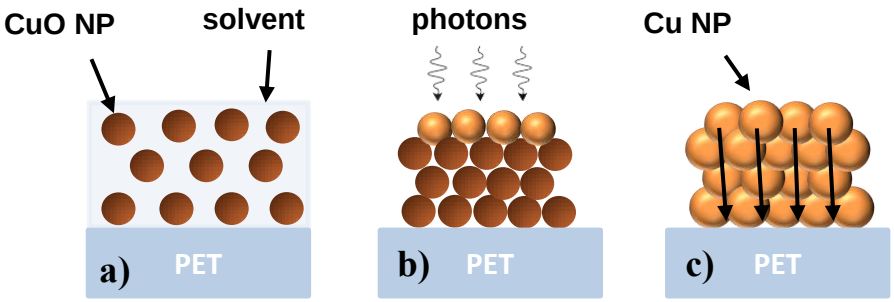

Figure 2. Schematic of the curing process: (a) 'as-printed' CuO ink, (b) film drying and beginning of photo-reduction, (c) continued chemical reduction and sintering of the ink to produce a conductive film.

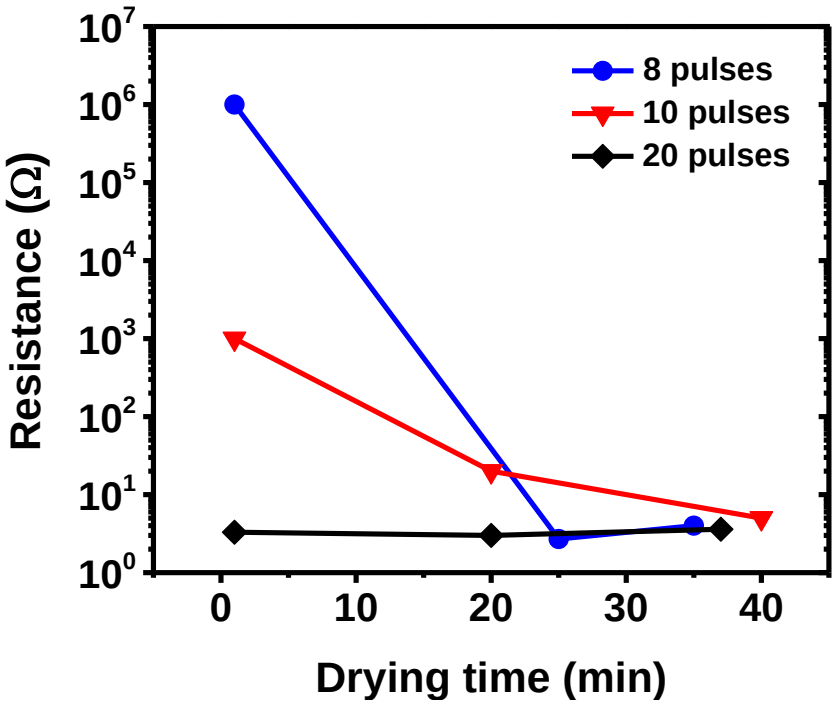

Figure 3. Dependence of print resistance on pre-sintering drying time in ambient air for a series of pulses (pulse duration: 2 ms).

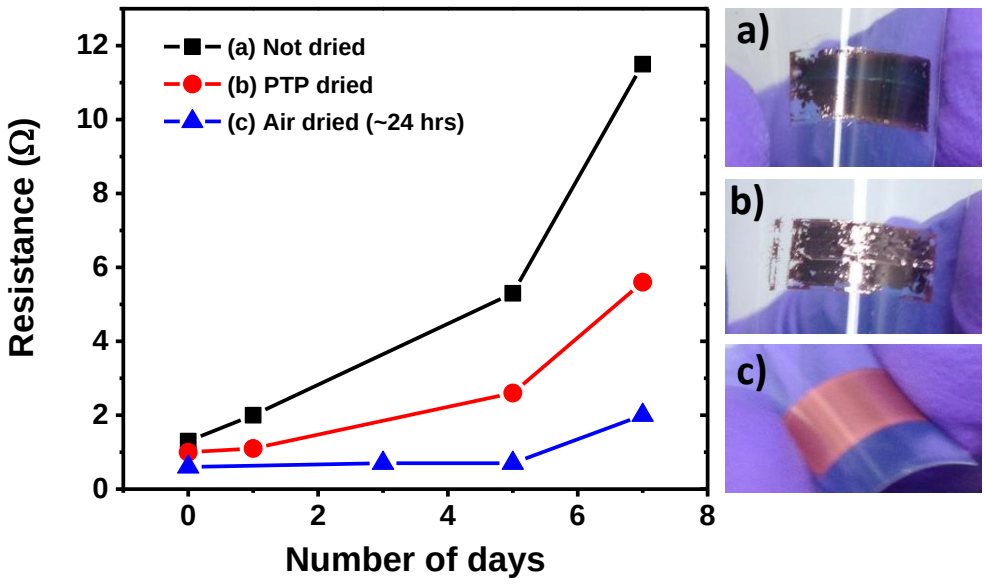

Figure 4. Changes in conductivity over the duration of one week in ambient atmosphere for undried, PTP dried, and air dried prints. All samples were sintered prior to air exposure using 2 pulses at 2 ms pulse duration. Right panel: Visual appearance of the same samples [(a) undried, (b) PTP dried, and (c) air dried] following one week of ambient atmosphere exposure. Note the dark coloration of the prints, in parts (a) and (b), is due to the oxidation of the Cu patterns.

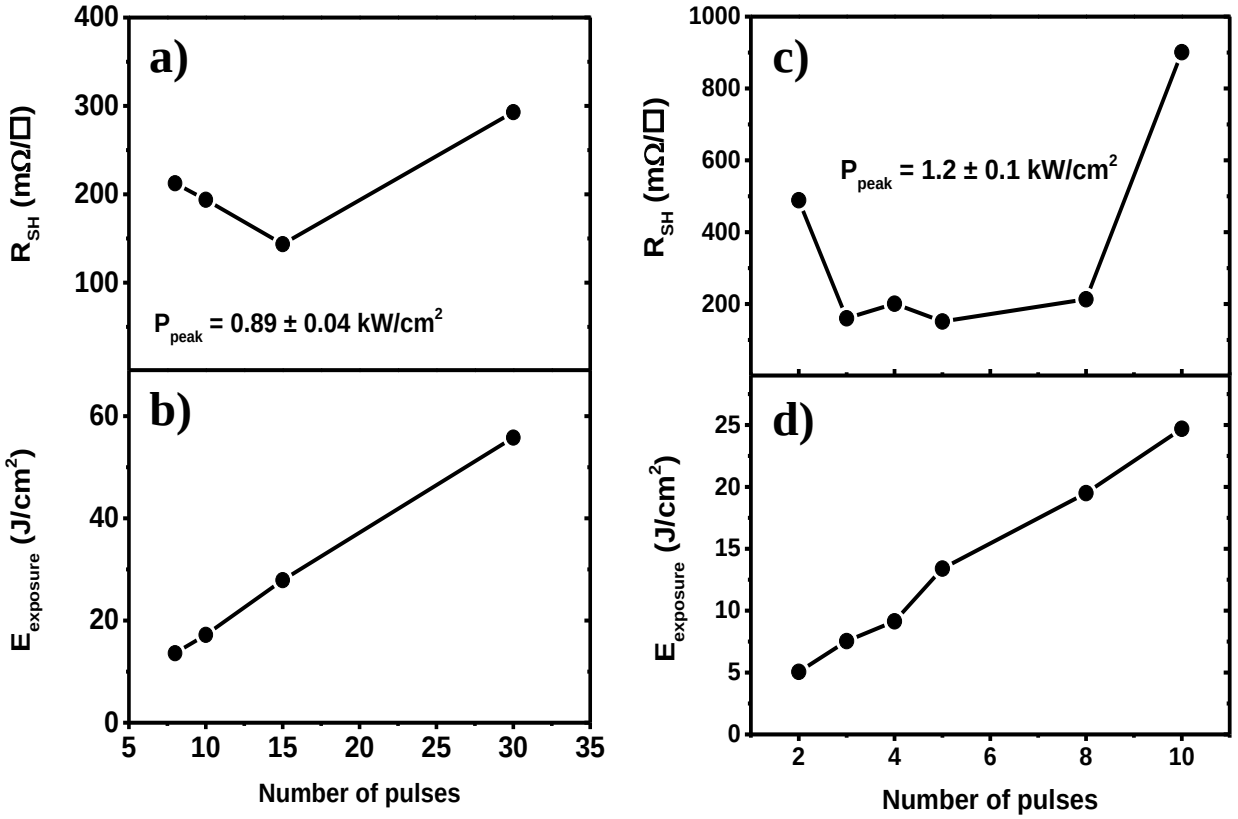

Figure 5. Sheet resistance and energy exposure values for varying number of pulses at two different peak power values [(a) and (b),0.89±0.04 kW/cm^2] –; [(c) and (d), 1.2±0.1 kW/cm^2]. The peak power was kept constant by controlling capacitor bank voltage and pulse width settings; 200V - 2ms (panels a,b) and 175V - 2ms (panels c,d).

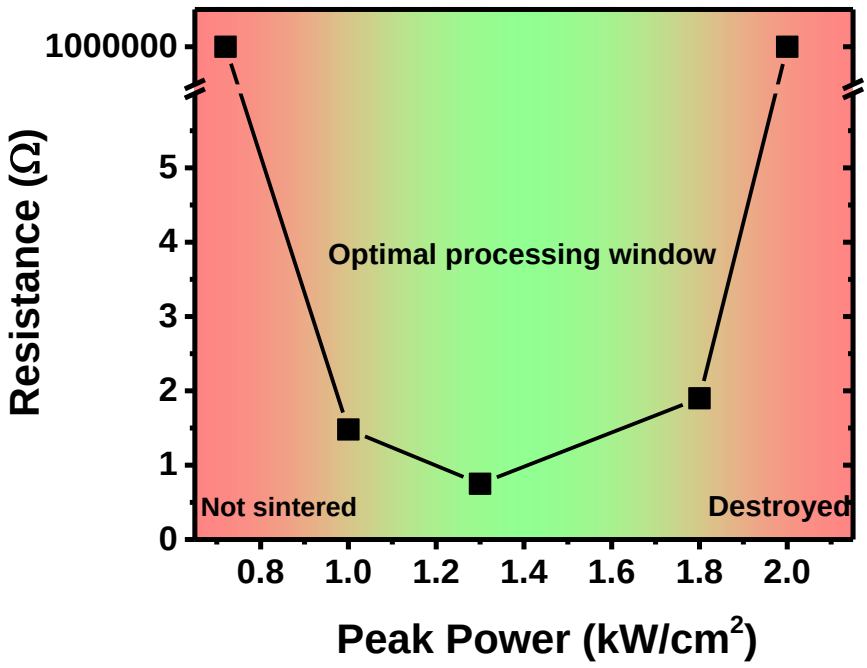

Figure 6. Changes in resistance as a function of peak power for a CuO ink sample sintered using 2 pulses at a constant $E_{exposure}$ of 10 J/cm^2.

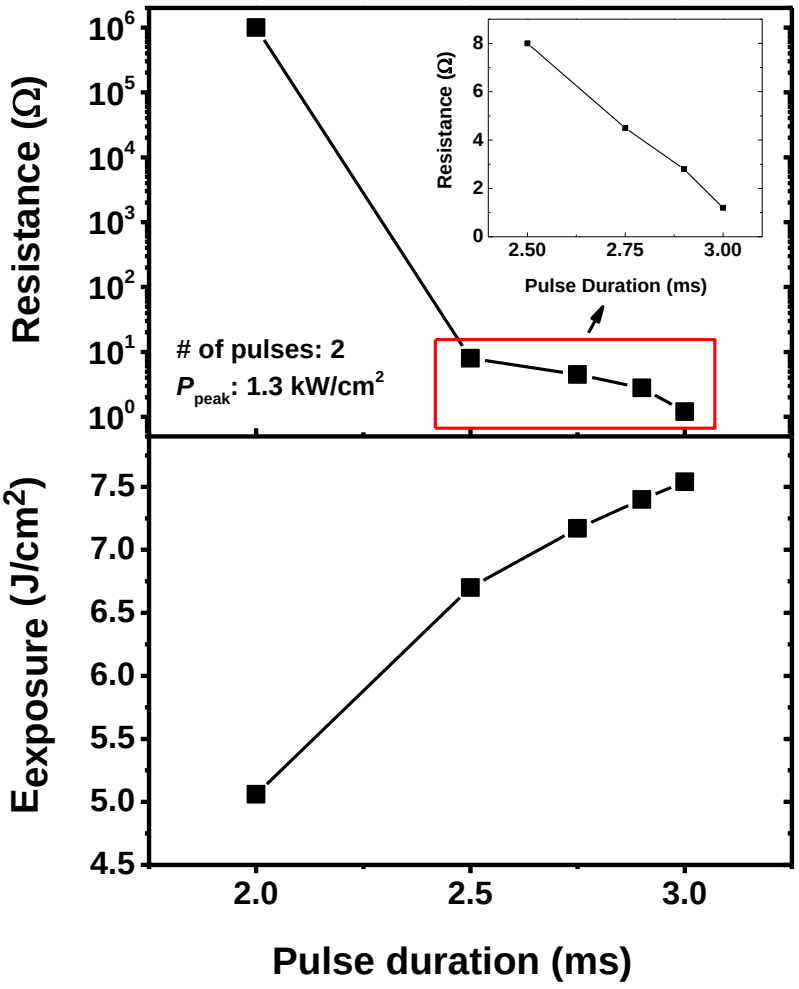

Figure 7. Resistance (top panel) and the corresponding energy exposure values (bottom panel) of samples sintered using 2 pulses at a constant P_{power} of 1.3 kW/cm^2 for varying pulse durations. The inset shows the values in the boxed region for more clarity.

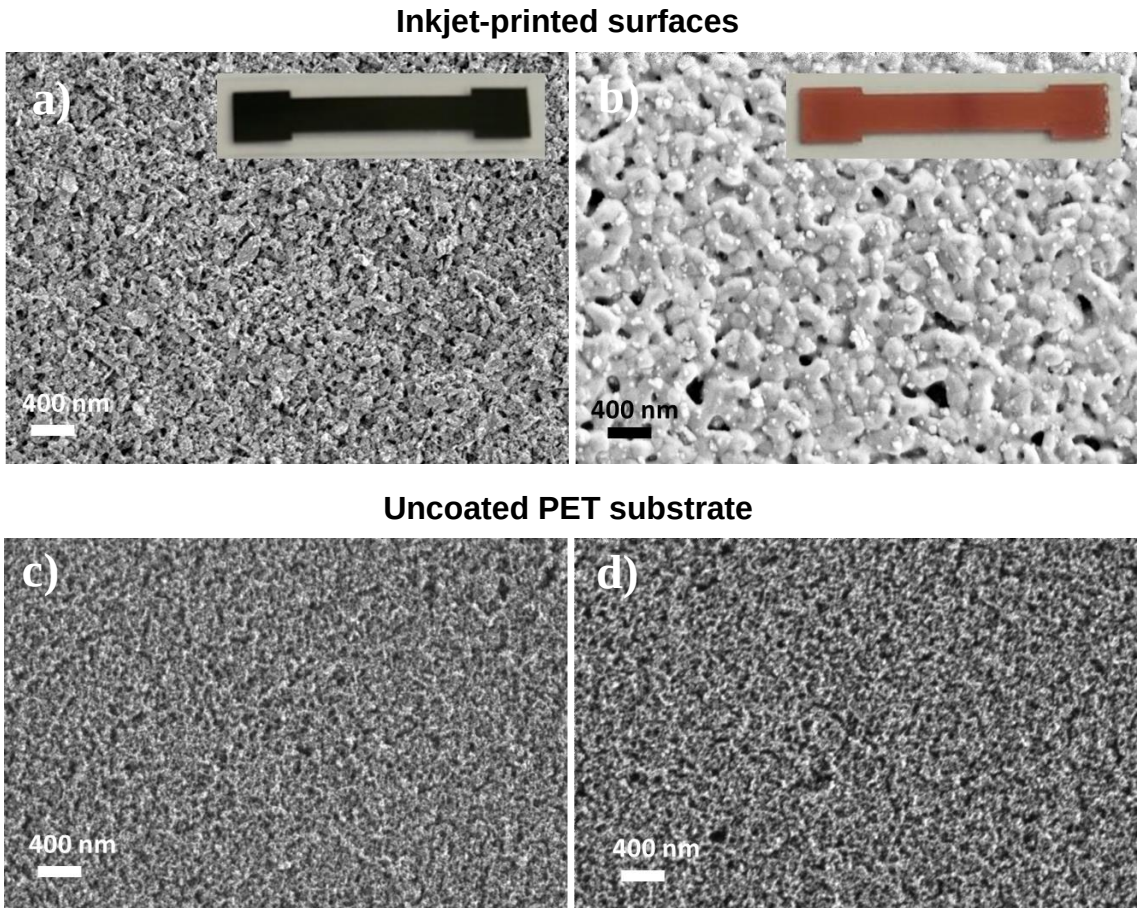

Figure 8. SEM images of (a) an 'as-printed' sample, (b) a sintered sample (2 pulses, pulse duration= 3.84ms, $E_{exposure}$ = 10 J/cm^2, P_{peak}= 1.3 kW/cm^2), (c) and (d) underlying PET substrate before and after PTP sintering via PTP, respectively. Insets correspond to the respective photographs of the actual ink-jet printed CuO (before sintering) and Cu (after sintering) patterns.

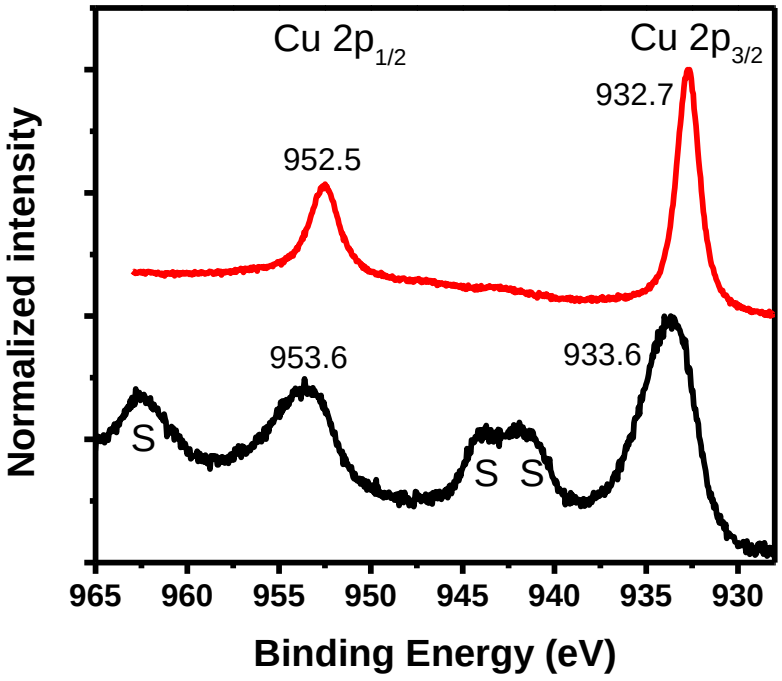

Figure 9. Cu 2p XPS data collected for the reduced (top trace) and as-cast films (bottom trace). The position of the Cu^{2+} shake-up lines[27] are denoted by (S).

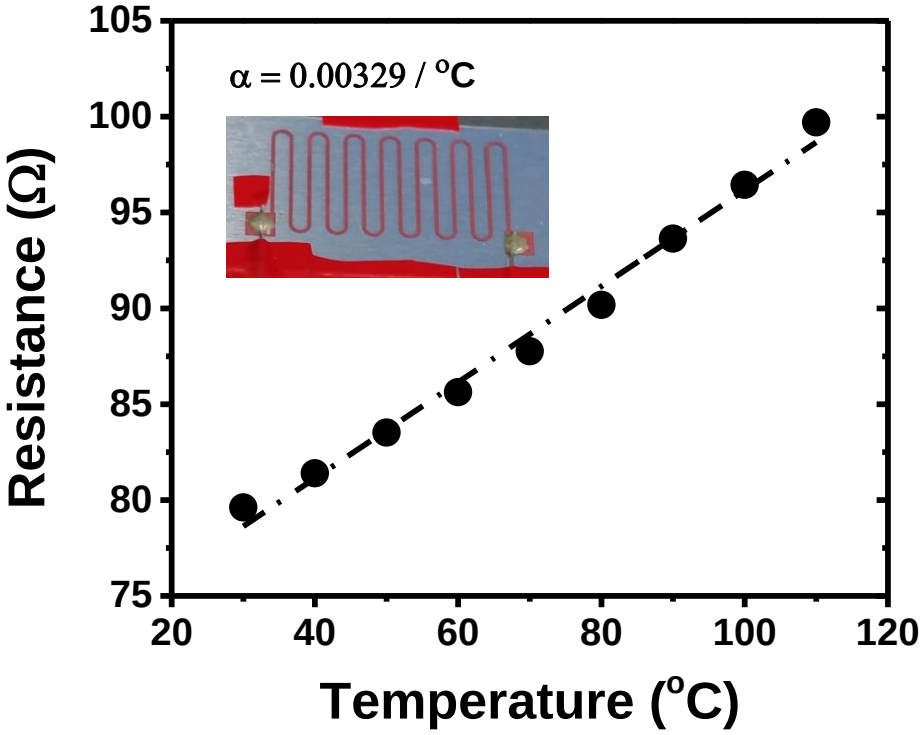

Figure 10. Dependence of ink-jet printed Cu sensor resistance as a function of temperature. Inset shows the actual printed device on flexible PET substrate. Dashed line represents the linear fit to the data.

ASSOCIATED CONTENT

Supporting Information

Simulated temperature profiles of CuO films at various photonic pulse durations. This material is available free of charge via the Internet at http://pubs.acs.org.

AUTHOR INFORMATION

Corresponding authors

*E-mail: aytugt@ornl.gov

*E-mail: joshipc@ornl.gov

Author Contributions

The manuscript was written through contributions of all authors. All authors have given approval to the final version of the manuscript. ‡These authors contributed equally.

Notes

The authors declare no competing financial interest.

ACKNOWLEDGEMENTS

This work was supported by the Laboratory Directed Research & Development program of Oak Ridge National Laboratory, managed by UT-Battelle, LLC for the U.S. Department of Energy. A portion of this research was supported by the Materials Sciences and Engineering Division, Office of Basic Energy Sciences, U.S. Department of Energy under contract with UT-Battelle, LLC (GMV – XPS). Support for Matt Rager is provided in part by the U.S. Department of Energy, Office of Science, Office of Workforce Development for Teachers and Scientists (WDTS) under the Science Undergraduate Laboratory Internship program.

REFERENCES

[1] Schroder, K. A. Mechanisms of photonic curing: Processing high temperature films on low temperatures substrates. *Nanotech. 2* **2011**, 2, 220-223.

[2] Zhang, T.; Wang, X.; Li, T.; Guo, Q.; Yang, J. Fabrication of flexible copper-based electronics with high-resolution and high-conductivity on paper via inkjet printing. *J. Mater. Chem. C.* **2014**, 2, 286-294.

[3] Öhlund, T.; Örtegren, J.; S Forsberg, S.; Nilsson, H. E.; Paper surfaces for metal nanoparticle inkjet printing. *Appl. Surf. Sci.* **2012**, 259, 731-739.

[4] Oprea, A.; Courbat, J.; Bârsan, N.; Briand, D.; de Rooij, N. F.; Weimar, U. Temperature, humidity and gas sensors integrated on plastic foil for low power applications. *Sens. Actuators, B.* **2009**, 140, 227-232.

[5] Ren, Y.; Virkki, J.; Sydänheimo, L.; Ukkonen, L. Optimisation of manufacturing parameters for inkjet-printed and photonically sintered metallic nanoparticle UHF RFID tags. *Electron. Lett.* **2014**, 50, 1504-1505.

[6] Søndergaard, R.; Hösel, M.; Angmo, D.; Larsen-Olsen, T. T.; Krebs F. C. Roll-to-roll fabrication of polymer solar cells. *Materials Today.* **2012**, 15, 36-49.

[7] Singh, M.; Haverinen, H. M.; Dhagat, P.; Jabbour, G. E. Inkjet printing-process and its applications. *Adv. Mater.* **2010**, *22*, 673.

[8] Lee, Y.; Choi, J.; Lee, K. J.; Stott, N. E.; Kim, D. Large-scale synthesis of copper nanoparticles by chemically controlled reduction for a
pplications of inkjet-printed electronics. *Nanotechnology*. **2008**, 19, 415604.

[9] Jin Sung Kang, Hak Sung Kim, Jongeun Ryu, H. Thomas Hahn, Seonhee Jang, Jae Woo Joung. Inkjet printed electronics using copper nanoparticle ink. *J. Mater. Sci.: Mater. Electron.* **2010**, 21, 1213-1220.

[10] Perelaer, J.; Abbel, R.; Wünscher, S.; Jani, R.; van Lammeren, T.; Schubert, U. S. Roll-to-Roll Compatible Sintering of Inkjet Printed Features by Photonic and Microwave Exposure: From Non-Conductive Ink to 40% Bulk Silver Conductivity in Less Than 15 Seconds. *Adv. Mater.* **2012**, 24, 2620–2625.

[11] Das, R.; Harrop, P. Printed, Organic & Flexible Electronics Forecasts, Players & Opportunities 2015-2025. *IDTechEx.* **2015**.

[12] Perelaer, J.; Smith, P. J.; Mager, D.; Soltman, D.; Volkman, S. K.; Subramanian, V.; Korvink, J. G.; Schubert, U. S. Printed electronics: the challenges involved in printing devices, interconnects, and contacts based on inorganic materials. *J. Mater. Chem*. **2010**, 20, 8446-8453.

[13] Kamyshny, A.; Magdassi, S. Conductive nanomaterials for printed electronics. *Small.* **2014**, 10, 3515-3535.

[14] Zenou, M.; Ermak, O.; Saar, A.; Kotler, Z. Laser sintering of copper nanoparticles. *J. Phys. D: Appl. Phys.* **2014**, 47, 025501.

[15] Ida, K.; Tomonari, M.; Sugiyama, Y.; Chujyo, Y.; Tokunaga, T.; Yonezawa, T.; Kuroda, K.; Sasaki, K. Behavior of Cu nanoparticles ink under reductive calcination for fabrication of Cu conductive film. *Thin Solid Films*. **2012**, 520, 2789-2793.

[16] Magdassi, S.; Grouchko, M.; Kamyshny, A. Copper nanoparticles for printed electronics: routes towards achieving oxidation stability. *Materials.* **2010**, 3, 4626-4638.

[17] Kang, B.; Han, S.; Kim, J.; Ko, S.; Yang, M. One-step fabrication of copper electrode by laser-induced direct local reduction and agglomeration of copper oxide nanoparticle. *J. Phys. Chem. C.* **2011**, 115, 23664-23670.

[18] Jin Sung Kang, Hak Sung Kim, Jongeun Ryu, H. Thomas Hahn, Seonhee Jang, Jae Woo Joung. Inkjet printed electronics using copper nanoparticle ink. *J. Mater. Sci.: Mater. Electron.* **2010**, 21, 1213-1220.

[19] Kang H.; Sowade E.; Baumann, R. R. Direct Intense Pulsed Light Sintering of Inkjet-Printed Copper Oxide Layers within Six Milliseconds. *ACS Appl. Mater. Interfaces*. **2014**, 6, 1682-1687.

[20] Joo, S. J.; Hwang, H. J.; Kim, H. S. Highly conductive copper nano/microparticles ink via flash light sintering for printed electronics. *Nanotechnology*. **2014**, 25, 265601.

[21] Niittynen, J.; Sowade, E.; Kang, H.; Baumann, R. R.; Mäntysalo, M. Comparison of laser and intense pulsed light sintering (IPL) for inkjet-printed copper nanoparticle layers. *Scientific reports*. **2015**, 5.

[22] Wu, J.; Liu, L.; Jiang, B.; Hu, Z.; Wang, X. Q.; Huang, Y. D.; Lin, D. R.; Zhang, Q. H. A coating of silane modified silica nanoparticles on PET substrate film for inkjet printing. *Appl. Surf. Sci.* **2012**, 258(12), 5131-5134.

[23] Liu, Yu-Feng; Tsai, Ming-Hsu; Pai, Yen-Fang; Hwang, Weng-Sing. Control of droplet formation by operating waveform for inks with various viscosities in piezoelectric inkjet printing. *Applied Physics A*. **2013**, 111, 509-516

[24] Paquet C.; James R.; Kell A. J.; Mozenson O.; Ferrigno J.; Lafrenière S.; Malenfant P. R. L. Photosintering and electrical performance of CuO nanoparticle inks. *Org. Electron*. **2014**, 15, 1836-1842.

[25] Li, J.; Mayer, W.; Colgan, E. G. Oxidation and protection in copper and copper alloy thin films. *J. Appl. Phys.***1991**, 70, 2820-2827.

[26] Lim, S.; Joyce, M.; Fleming, P. D.; Aijazi, A. T.; Atashbar, M. Inkjet Printing and Sintering of Nano-Copper Ink. *J. Imaging Sci. Technol*. **2013**, 57, 50506-1-50506-7(7) .

[27] Biesinger, M. C.; Lau, L. W. M.; Gerson, A. R.; Smart, R. St. C. Resolving surface chemical states in XPS analysis of first row transition metals, oxides and hydroxides: Sc, Ti, V, Cu and Zn. *Appl. Surf. Sci*. **2010**, 257, 887-898.

[28] Giancoli, D. Physics for Scientists and Engineers with Modern Physics; Phillips, J., Eds.; 4th ed; Prentice Hall: Upper Saddle River, New Jersey Chapter 25, p 658.

[29] Mayadas, A.; Shatzkes, M. Electrical-resistivity model for polycrystalline films: the case of arbitrary reflection at external surfaces. *Phys. Rev. B.* **1970**, 1, 1382.

TABLE OF CONTENTS